Article

A Density Functional Theory Investigation on the Mechanism of the Second Half-Reaction of Nitric Oxide Synthase

Jesse J. Robinet, Kyung-Bin Cho, and James W. Gauld

More About This Article

Additional resources and features associated with this article are available within the HTML version:

- Supporting Information
- Access to high resolution figures
- Links to articles and content related to this article
- Copyright permission to reproduce figures and/or text from this article

View the Full Text HTML

A Density Functional Theory Investigation on the Mechanism of the Second Half-Reaction of Nitric Oxide Synthase

Jesse J. Robinet, Kyung-Bin Cho,[†] and James W. Gauld*

Department of Chemistry and Biochemistry, University of Windsor, Windsor, Ontario N9B 3P4, Canada

Received April 16, 2007; E-mail: gauld@uwindsor.ca

Abstract: Density functional theory methods have been employed to systematically investigate the overall mechanism of the second half-reaction of nitric oxide synthases. The initial heme-bound hydrogen peroxide intermediate previously identified is found to first undergo a simple rotation about its O−O peroxide bond. Then, via a "ping-pong" peroxidase-like mechanism the −O$_{in}$H− proton is transferred back onto the substrate's −NO oxygen then subsequently onto the outer oxygen of the resulting Fe$_{heme}$−OOH species. As a result, O$_{out}$ is released as H$_2$O with concomitant formation of a compound I-type (Fe$_{heme}$−O) species. Formation of the final citrulline and NO products can then be achieved in one step via a tetrahedral transition structure resulting from direct attack of the Fe$_{heme}$−O moiety at the substrate's guanidinium carbon center. The possible role of alternative mechanisms involving a protonated compound II-type species or an initial transfer of only the −NH− hydrogen of the =NHOH$^+$ group of N^ω-hydroxy-L-arginine is also discussed.

1. Introduction

Nitric oxide (NO) is an important biosignalling molecule that has been found to play key roles in a diverse range of physiological processes including neurotransmission, blood pressure regulation, and the immune system.[1−4] Consequently, there is considerable and increasing interest in better understanding its biological chemistry, in particular elucidating the enzymatic mechanism(s) by which it may be synthesized in vivo.

Within mammals[5,6] NO is synthesized by the class of enzymes known as the nitric oxide synthases (NOSs). Three NOS isozymes are known: neuronal, endothelial, and inducible (iNOS).[6−8] Importantly, while they do differ from each other, they have all been found to possess similar structures and require the same cofactors. For example, each isozyme can be generally divided into an N-terminal reductase and a C-terminal oxygenase domain. The former is responsible for donating electrons to the active site during the reaction and binds the cofactors nicotinamide adenine dinucleotide phosphate (NADPH), flavin adenine dinucleotide, and flavin mononucleotide.[8−10] The latter

domain contains the active site itself within which is bound a heme group via a cysteine residue while a tetrahydrobiopterin (H$_4$B) moiety binds adjacent to a propionate arm of the heme.[7,8] Significantly, however, all three isozymes possess a highly conserved active site. Consequently, they are all believed to produce NO via the same enzymatic mechanism in which an arginine is sequentially oxidized via two half-reactions to give citrulline and NO, as illustrated in Scheme 1.
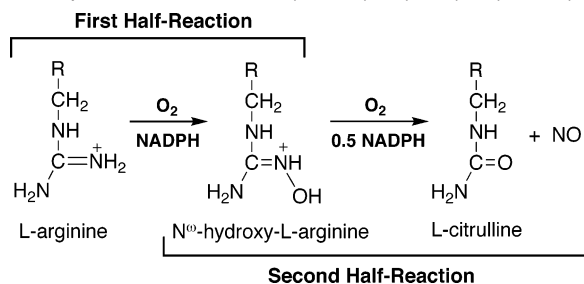
In the first half-reaction, the arginine is oxidized to give N^ω-hydroxy-L-arginine (NHA). This is generally thought to occur via a mechanism analogous to that of P450-like oxidase enzymes. That is, it is thought to proceed via a compound I-type intermediate and effectively results in the insertion of an oxygen into an X−H bond with consumption of an O$_2$ and two electrons from NADPH.[8,11−13] In the second half-reaction, the resulting NHA is oxidized to give citrulline and NO. This again requires one O$_2$, but now consumes just one additional electron (Scheme 1). However, there appears to be no currently known analogous enzymatic mechanism for this half-reaction. As a result, it has been the subject of a number of detailed experimental investigations. On the basis of the results obtained, several mechanisms have been proposed and reviewed in detail elsewhere.[8,11,14−20]

[†] Current Address: Department of Organic Chemistry and the Lise Meitner-Minerva Center for Computational Quantum Chemistry, The Hebrew University of Jerusalem, 91904 Jerusalem, Israel.

(1) Kerwin, J. F., Jr.; Lancaster, J. R., Jr.; Feldman, P. L. *J. Med. Chem.* **1995**, *38*, 4343.
(2) Garthwaite, J.; Boultan, C. L. *Annu. Rev. Physiol.* **1995**, *57*, 683.
(3) Schmidt, H. H. H. W.; Walter, U. *Cell* **1994**, *78*, 919.
(4) Nath, A. K.; Madri, J. A. *Dev. Biol.* **2006**, *292*, 25.
(5) Stuehr, D. J. *Biochem. Biophys. Acta* **1999**, *1411*, 217.
(6) Knowles, R. G.; Moncada, S. *Biochemistry J.* **1994**, *298*, 249.
(7) Wei, C.-C.; Crane, B. R.; Stuehr, D. J. *Chem. Rev.* **2003**, *103*, 2365.
(8) Alderton, W. K.; Cooper, C. E.; Knowles, R. G. *Biochemistry J.* **2001**, *357*, 593.
(9) Guan, Z.-W.; Kamatani, D.; Kimura, S.; Iyanagi, T. *J. Biol. Chem.* **2003**, *278*, 30859.
(10) Jachymova, M.; Martasek, P.; Panda, S.; Roman, L. J.; Panda, M.; Shea, T. M.; Ishimura, Y.; Kim, J.-J. P.; Masters, B. S. S. *Proc. Natl. Acad. Sci. U.S.A.* **2005**, *102*, 15833.

(11) Griffith, O. W.; Stuehr, D. J. *Annu. Rev. Physiol.* **1995**, *57*, 707.
(12) Stuehr, D. J.; Santolini, J.; Wang, Z.-Q.; Wei, C.-C.; Adak, S. *J. Biol. Chem.* **2004**, *279*, 36167.
(13) Crane, B. R.; Arvai, A. S.; Ghosh, D. K.; Wu, C.; Getzoff, E. D.; Stuehr, D. J.; Tainer, J. A. *Science* **1998**, *279*, 2121.
(14) Crane, B. R.; Arvai, A. S.; Ghosh, S.; Getzoff, E. D.; Stuehr, D. J.; Tainer, J. A. *Biochemistry* **2000**, *39*, 4608.
(15) Rusche, K. M.; Spiering, M. M.; Marletta, M. A. *Biochemistry* **1998**, *37*, 15503.
(16) Clague, M. J.; Wishnok, J. S.; Marletta, M. A. *Biochemistry* **1997**, *36*, 14465.
(17) Korth, H.-G.; Sustmann, R.; Thater, C.; Butler, A. R.; Ingold, K. U. *J. Biol. Chem.* **1994**, *269*, 17776.
(18) Marletta, M. A. *J. Biol. Chem.* **1993**, *268*, 12231.
(19) Rosen, G. M.; Tsai, P.; Pou, S. *Chem. Rev.* **2002**, *102*, 1191.

Scheme 1. Overall Mechanism Catalyzed by NOSs Illustrating Its Two Component Half-Reactions (R = −(CH₂)₂CH(NH₂)COOH)

First Half-Reaction

L-arginine → (O₂, NADPH) → N^ω-hydroxy-L-arginine → (O₂, 0.5 NADPH) → L-citrulline + NO

Second Half-Reaction

Scheme 2. Summary of Common Features of the Various Proposed Mechanisms for the Second Half-Reaction in Which NO Is Formed via a Tetrahedral Intermediate
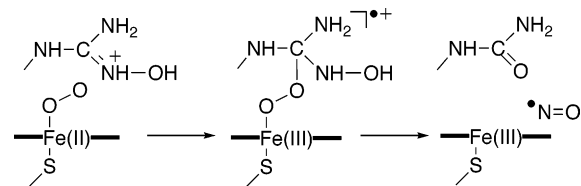
a Note: proposed ionization and protonation states may vary.

Unfortunately, due to the elusiveness of intermediates to experimental observation beyond an Fe_{heme}−OO⁻ species[21] and uncertainties about the nature of the NHA substrate, the exact mechanism remains unclear. Indeed, it was initially thought that the mechanistically key −NOH group of NHA was unprotonated. However, recent experimental[22] and computational[23,24] studies have suggested that it is in fact more likely protonated, i.e., −NHOH⁺. Nevertheless, while the proposed mechanisms differ with respect to key details, they generally share some common features, summarized in Scheme 2. In particular, the second half-reaction is accepted to begin with binding of an O_2 at the heme iron (Fe_{heme}) with addition of an electron. The resulting Fe_{heme}−O_2 species (or a derivative) is thought to then attack the NHA (or a derivative) at its guanidinium carbon (C_{guan}). The resulting "tetrahedral" species containing a peroxo Fe_{heme}−O−O−C_{guan} link is proposed to then react further to ultimately give citrulline and NO.

Recently, we[25] performed a computational investigation that examined a variety of previously proposed tetrahedral derivatives containing an Fe_{heme}−O−O−C_{guan} cross-link as well as possible alternatives. Importantly, the results suggested that such species most likely lie too high in energy to be mechanistically feasible. In addition, we also considered various possible initial steps that may occur once the O_2 is bound to the heme. Intriguingly, it was found that the most likely initial step involves the transfer of both hydrogens from the substrate's protonated −NHOH⁺ group to the Fe_{heme}−O_2 moiety to give a heme-bound hydrogen peroxide, i.e., Fe_{heme}−(H)OOH. Such an initial reaction step had not previously been proposed for the second half-reaction of NOS. Furthermore, the resulting Fe_{heme}−

Scheme 3. Schematic Depiction of the Active Site of NOS as Modeled in This Study*a*
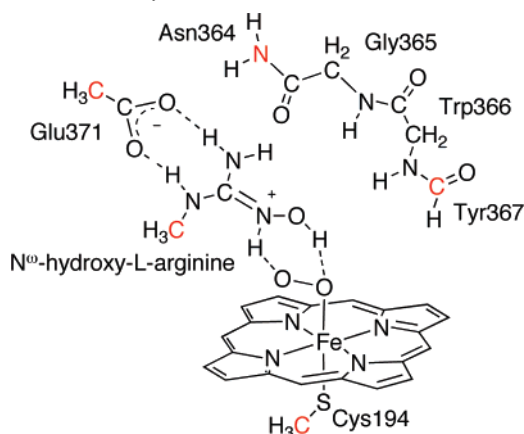
a Atoms highlighted in red were held fixed in the crystal structure position throughout the optimizations.

(H)OOH intermediate was calculated to be almost thermoneutral with the initial reactants, lying just marginally higher in energy.[25]

In this present study, we have employed density functional theory (DFT) methods to investigate the complete mechanism for the second half-reaction of nitric oxide synthases.

2. Computational Methods

All calculations were performed using the hybrid DFT method B3LYP, a combination of Becke's three-parameter hybrid exchange functional[26] with the Lee−Yang−Parr correlation functional[27] as implemented in *Gaussian 03*[28] and *Jaguar 5.5*.[29] Optimized structures and frequencies were obtained using the LACVP basis set on all atoms except sulfur, for which LACV3P** was used. General effects due to the polarity of the protein environment (solvation correction) were modeled by performing single point calculations at the above level of theory on the optimized structures, using the Poisson−Boltzmann−PCM method with a dielectric constant (ϵ) of 4.0. Relative energies were obtained by performing single point calculations using the larger LACV3P** basis set on all atoms, i.e., at the B3LYP/LACV3P** level of theory, with inclusion of the appropriate solvation correction (ΔE^{solv}). Spin density values mentioned in the text were obtained at the above higher level of theory.

The active site was modeled as previously reported[25] based on the iNOS crystal structure PDB: 1DWX[14] (Scheme 3). Specifically, the heme was modeled as a Fe-porphyrin with a thiolmethyl anion as the axial Cys194, while the active site residue Glu371 was modeled as an acetate. The substrate NHA has been modeled by 1-methyl-2-hydroxy-guanidinium. The protein backbone between the carboxylate carbon of Asn364 and the amide nitrogen of Tyr367 has also been included. As described in our previous study,[25] the initial oxidation state of the [porphyrin−Fe^{III}−O_2] group was set to zero. As a result the total charge of the system is −1. In order to maintain the integrity of the protein's active site, a minimal number of terminal atoms were held fixed according to their positions in the above crystal structure (highlighted in red in Scheme 3 and marked by an X in all Figures). See also ref 25 for further details.

We have previously successfully employed the above methods and models to the study of the binding of NHA within the iNOS active site[24] and to the study of possible tetrahedral intermediates and initial steps in the second half-reaction of NOSs.[25] The applicability of such

(20) Huang, H.; Hah, J.-M.; Silverman, R. B. *J. Am. Chem. Soc.* **2001**, *123*, 2674.
(21) Davydov, R.; Ledbetter-Rogers, A.; Martásek, P.; Larukhin, M.; Sono, M.; Dawson, J. H.; Masters, B. S. S.; Hoffman, B. M. *Biochemistry* **2002**, *41*, 10375.
(22) Tierney, D. L.; Huang, H.; Martásek, P.; Roman, L. J.; Silverman, R. B.; Masters, B. S. S.; Hoffman, B. M. *J. Am. Chem. Soc.* **2000**, *122*, 5405.
(23) Tantillo, D. J.; Fukuto, J. M.; Hoffman, B. M.; Silverman, R. B.; Houk, K. N. *J. Am. Chem. Soc.* **2000**, *122*, 536.
(24) Cho, K.-B.; Gauld, J. W. *J. Am. Chem. Soc.* **2004**, *126*, 10267.
(25) Cho, K. B.; Gauld, J. W. *J. Phys. Chem. B* **2005**, *109*, 23706.

(26) Becke, A. D. *J. Chem. Phys.* **1993**, *98*, 1372.
(27) Lee, C.; Yang, W.; Parr, R. G. *Phys. Rev. B: Condens. Matter Mater. Phys.* **1988**, *37*, 785.
(28) Frisch, M. J. et al. *Gaussian 03*; Gaussian, Inc.: Wallingford, CT, 2004. See Table S3 of the Supporting Information for the complete citation.
(29) Schrodinger, L. L. C. In *Jaguar 5.5*; Portland, OR, 1991−2003.

computational approaches to the study of related enzymatic systems has also been previously discussed.[30]

3. Results and Discussion

3.1. Substrate-Bound Active Site and Initial Reaction Step. As noted in the Introduction, we have previously employed computational methods to investigate the binding of the substrate (NHA) within the active site with an O_2 moiety simultaneously bound to the Fe_{heme} center.[24] The structure is shown schematically in Scheme 3 and is hereafter referred to as the "bound active site" (**1**). In addition, we also examined a variety of possible initial steps for the second half-reaction.[25] In order to assist in placing the present results into context, the most relevant findings from these previous computational studies are summarized here. In particular:

(i) The lowest energy bound active site structure (**1**) was found[24] to correspond to the $-NHOH^+$ group of NHA forming two hydrogen bonds with the Fe-bound O_2 ($Fe_{heme}-O_2$). Specifically, the $-OH$ and $-NH-$ groups form hydrogen bonds with the inner (O_{in}) and outer (O_{out}) oxygens of the $Fe_{heme}-O_{in}-O_{out}$ group, respectively (see Scheme 3).

(ii) The lowest energy state of **1** has a multiplicity (multi) of 1, i.e., **1**^{1}.[24]

(iii) The initial step of the second half-reaction was found to most likely be the concomitant transfer of both hydrogens from the $-NHOH^+$ group to the O_2 moiety via the transition structure **TS1** with a relative energy barrier (multi = 1) of 14.8 kcal mol^{-1}.[25] Furthermore, the resulting Fe_{heme}-bound hydrogen peroxide ($Fe_{heme}-(H)OOH$) intermediate (**2**) was found to be remarkably low in energy with its singlet (**2**^{1}) and triplet states (**2**^{3}) lying higher in energy than **1**^{1} by just 2.4 and 2.0 kcal mol^{-1}, respectively.[25]

In this present study, the relative energies of the singlet and triplet states of the intermediates and transition structures encountered were generally found to lie quite close in energy and, furthermore, lower than that of higher multiplicities. Thus, all relative energies mentioned herein refer to the multi = 1 and 3 states unless otherwise noted (see also Table S2, Supporting Information). In addition, the structures of both states exhibit the same general features. Thus, only those of the singlets are shown herein while those of the corresponding triplets and higher multiplicities, where appropriate, are given in Table S1 (Supporting Information).

3.2. Possible Reactions of the $Fe_{heme}-(H)OOH$ Intermediate. In this present study, we began by systematically considering possible reaction pathways for the Fe_{heme}-bound hydrogen peroxide species **2**. The schematic potential energy surfaces (PESs) obtained are shown in Figure 1 while the optimized structures of the resulting singlet state transition structures and intermediates are shown in Figure 2.

As noted previously, the relative energies of the singlet and triplet states of **2** (**2**^{1} and **2**^{3}) are quite close with the triplet lying just 0.4 kcal mol^{-1} lower in energy (Figure 1).[25] For both states, the lowest energy reaction path was found to correspond to rotation about the peroxide O−O bond. This conformational change proceeds via **TS2**^{1} and **TS2**^{3} with essentially equal barriers of just 1.5 and 1.6 kcal mol^{-1}, respectively. The singlet

(30) (a) Blomberg, M. R. A.; Siegbahn, P. E. M. *J. Phys. Chem. B* **2001**, *105*, 9375. (b) Siegbahn, P. E. M.; Blomberg, M. R. A. *Chem. Rev.* **2000**, *100*, 421. (c) Siegbahn, P. E. M. *J. Comput. Chem.* **2001**, *22*, 1634. (d) Himo, F.; Siegbahn, P. E. M. *Chem. Rev.* **2003**, *103*, 2421.
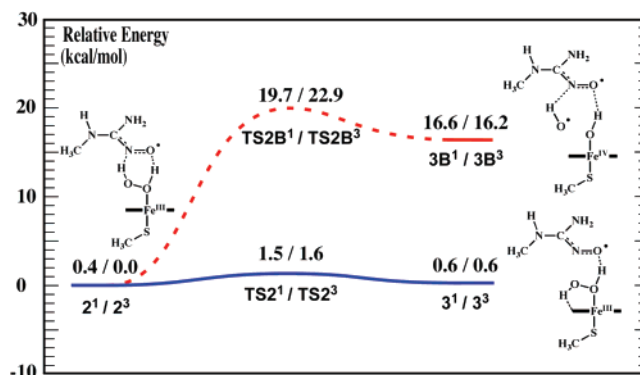
Figure 1. Schematic potential energy surfaces obtained for possible reactions of the $Fe_{heme}-(H)O-OH$ intermediate **2**. Relative energies are shown in kcal mol^{-1}.
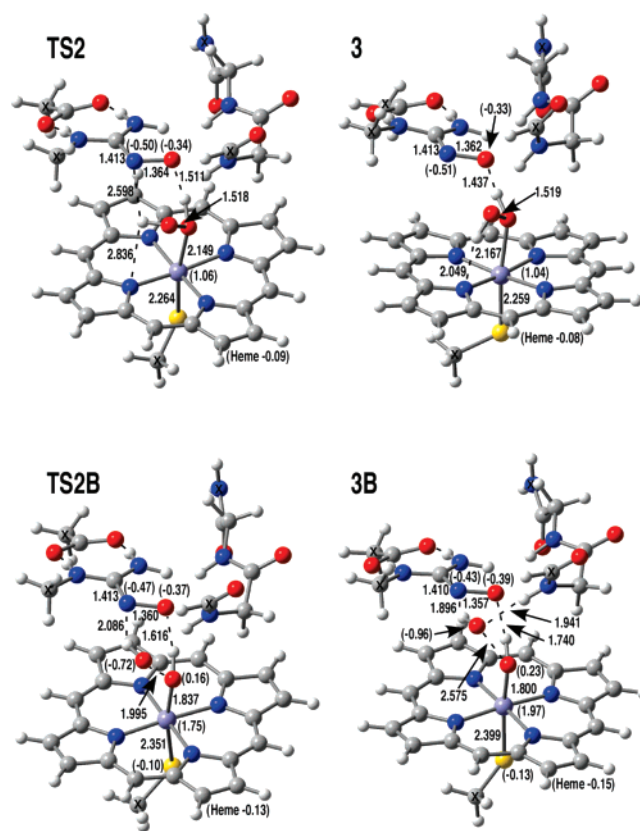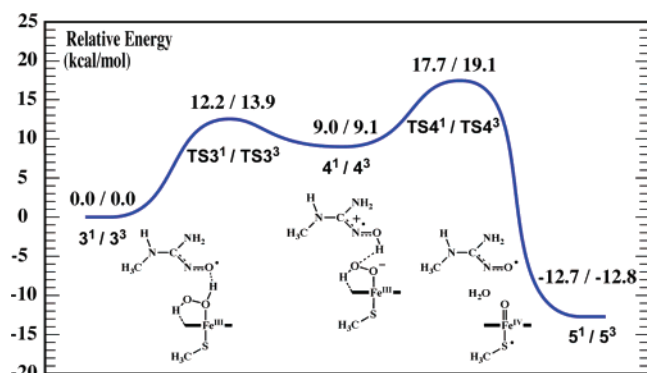

Figure 2. Optimized structures of the singlet state intermediates and transition structures shown in Figure 1 arising from the reaction of the $Fe_{heme}-(H)O-OH$ intermediate **2**. Selected optimized distances (Å) and spin densities (in parentheses) are also shown. Color key: Fe (purple); S (yellow); C (gray); N (blue); O (red); H (white).

(**3**^{1}) and triplet (**3**^{3}) states of the resulting alternate $Fe_{heme}-(H)O-OH$ conformer **3** are very close in energy. Importantly, however, they are both just 0.6 kcal mol^{-1} higher in energy than **2**^{3}. In both, the $-O_{out}H$ group is now directed down toward a nitrogen of the porphyrin (N_{heme}) with an $-O_{out}H\cdots N_{heme}$ interaction distance in **3**^{1} of 2.049 Å (Figure 2). However, the $-O_{in}H-$ group remains hydrogen bonded to the oxygen of the substrate's $-NO$ group although now it is considerably shorter. For example, its length in **3**^{1} is just 1.437 Å (see Figure 2), a decrease of 0.501 Å from that observed for the corresponding intermediate **2**^{1}.[25]

Figure 3. Schematic potential energy surface for the formation of compound I from the $Fe_{heme}-(H)O-OH$ intermediate **3**. Relative energies are shown in kcal mol^{-1}.

Due to the fact that $3^1/3^3$ differ from $2^1/2^3$ simply by rotation about the O−O bond, their spin and charge distributions are very similar (Figure 2). For example, in 3^1 the calculated spin on the formally Fe(III) center is 1.06 (cf. 1.02 in 2^1)[25] while a radical is again predominantly located on the substrates −NO group (−0.82).

A potential alternate pathway was also examined in which the $Fe_{heme}(H)O-OH$ bond undergoes homolytic cleavage to give an $Fe_{heme}-OH$ species and an •OH radical and is shown in Figure 1 (red-dashed line). An analogous reaction step for an $Fe_{heme}-OOH$ species has been previously considered in the mechanism of cytochrome P450cam.[31] However, in the present system such a reaction proceeds via **TS2B** with high barriers of 19.7 and 22.9 kcal mol^{-1} for the singlet and triplet states, respectively (Figure 1). Importantly, these barriers are markedly higher than those of the above "rotation pathway" and thus will not be competitive. Furthermore, the resulting intermediates $3B^1$ and $3B^3$ lie significantly higher in energy than 2^3 by 16.6 and 16.2 kcal mol^{-1}, respectively (Figure 1). We note that in **3B** a radical is again formally located on the substrates −NO group (spin density: −0.82) while another is now also found on the cleaved hydroxyl (spin density: −0.97). In addition, the hydroxy-ferryl group resembles a previously[32] described protonated compound II species (ie., $Fe^{IV}-OH^+$) with Fe and O spin densities of 1.97 and 0.29 and an Fe−O bond length of 1.800 Å (Figure 2). As cleavage of the O−O bond is not competitive with rotation about the same bond, this alternate pathway is not discussed further.

3.3. Formation of "Compound I" from $Fe_{heme}-(H)OOH$ Intermediate 3. We then considered possible reactions of the $Fe_{heme}-(H)OOH$ containing intermediate **3**. The reaction PES obtained is shown in Figure 3 while optimized structures of the various singlet state intermediates and transition structures are shown in Figure 4. As for the lower energy $Fe_{heme}-(H)$-OOH conformer **2**, **3** could also alternately undergo homolytic cleavage at its O−O bond to give a protonated compound II-type complex. However, such a pathway was found to have similarly high barriers as noted for **2** of approximately 18 kcal mol^{-1} and higher (not shown). Hence, such a reaction is again unlikely to be competitive.

Rather, the lowest energy pathway other than rearrangement back to **2** corresponds to transfer of the heme-peroxides −O_{in}H−

(31) Zheng, J.; Wang, D.; Thiel, W.; Shaik, S. *J. Am. Chem. Soc.* **2006**, *128*, 13204.
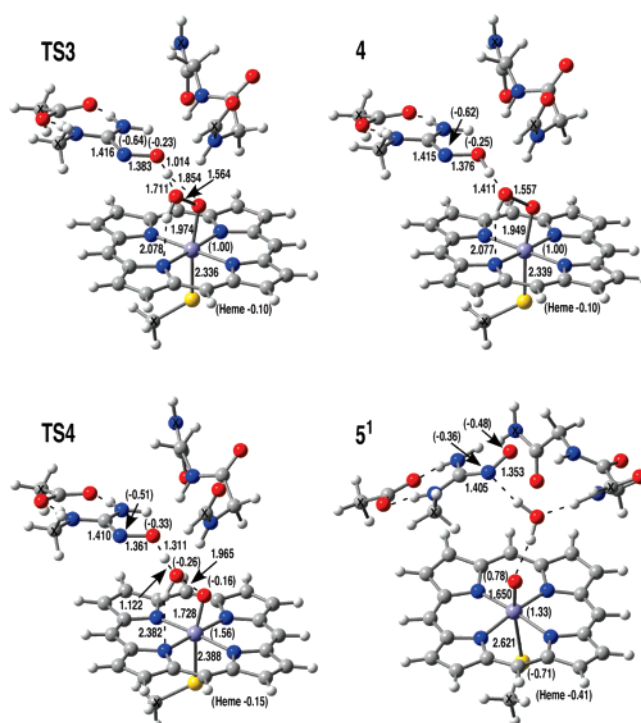(32) Derat, E.; Shaik, S. *J. Am. Chem. Soc.* **2006**, *128*, 8185.

Figure 4. Optimized structures of the singlet state intermediates and transition structures shown in Figure 3 arising from the reaction of the $Fe_{heme}-(H)O-OH$ intermediate **3**. Selected optimized distances (Å) and spin densities (in parentheses) are also shown. Color key: Fe (purple); S (yellow); C (gray); N (blue); O (red); H (white).

proton back onto the substrate's −NO• oxygen. This reaction proceeds via **TS3^1** and **TS3^3** at a cost of 12.2 and 13.9 kcal mol^{-1}, respectively, with the singlet pathway being slightly preferred (Figure 3). The singlet (4^1) and triplet (4^3) states of the resulting intermediate **4** lie quite close in energy and just 9.0 and 9.1 kcal mol^{-1}, respectively, higher in relative energy than **3**. On the basis of the calculated spin densities and optimized structural parameters (Figure 4) the heme-oxy species within **4** resembles $Fe^{III}_{heme}-O(^-)OH$ while the substrate derivative now contains a terminal $=NOH^{•+}$ group with the radical being more localized on the nitrogen center. Notably, the $Fe_{heme}O-OH$ bond has lengthened slightly. For example, the O−O bond in 4^1 is 0.038 Å longer than that observed for 3^1 (cf. Figure 2). Importantly, however, as can be seen in Figure 4 the substrate's resulting $=NOH^{•+}$ moiety does not maintain a hydrogen bond with the $Fe_{heme}-O_{in}-$ oxygen. Instead, the $=NOH^{•+}$ hydroxyl now in fact forms a quite short hydrogen bond with the *outer* oxygen (O_{out}) of the $Fe^{III}_{heme}-O(^-)OH$ moiety.

Interestingly, **4** in essence corresponds to transfer of just the $=NH-$ hydrogen of the initial NHA substrate's $=NHOH^+$ moiety to $-O_{out}$ of the initial $Fe_{heme}-O_2$ species. It should be noted that in our previous[25] computational examination of possible first steps in the second half-reaction of NOS we obtained an intermediate arising directly from the bound active site **1** by just such a transfer (**2** in ref 25). However, it differed from **4** above in that the resulting $-O_{out}H$ group was hydrogen bonded to the substrate's $=NOH^{•+}$ nitrogen while concomitantly the $=NOH^{•+}$ hydroxyl was hydrogen bonded to $-O_{in}-$ of the $Fe_{heme}-OOH$ moiety.[25] Furthermore, it was decidedly higher in energy than 4^1 above by >6 kcal mol^{-1}. In addition, it was found to be thermodynamically and kinetically unstable with
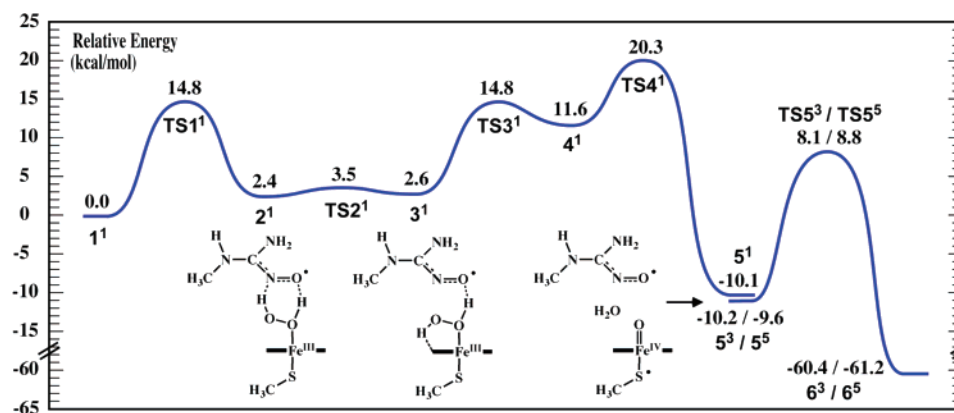
Figure 5. Schematic potential energy surface for the overall mechanism of the second half-reaction of NOSs. Relative energies are shown in kcal mol^{-1}.

respect to rearrangement back to **1**. However, the above results suggest a possible higher energy pathway that could still lead to formation of an intermediate **4**-type species.[25] Specifically, transfer of the substrate's =NH— hydrogen to —O$_{out}$ of the Fe$_{heme}$—O$_2$ moiety to give the previous high-energy intermediate, presumably followed by rotation about the resulting Fe$^{III}_{heme}$O—OH bond and a hydrogen bond interaction shift from NOH···O$_{in}$ to NOH···O$_{out}$. Notably, previous experimental studies have suggested that NO formation still occurs, though at a reduced rate, when substrate analogues lacking the —OH proton are used.[28] This possible alternate higher energy pathway may help to explain how •NO may still be formed in such cases, though without the final interaction shift.

As noted above, in the =NOH•+ group of **4** the radical is calculated to be more centered on the nitrogen (−0.62) with some delocalization to the oxygen (−0.25) as shown in Figure 4. Interestingly, a previous[23] combined computational and experimental study considered the protonation state of the initial NHA substrate, and significantly, the nature of possible oxygen- or nitrogen-centered radicals that may be formed during the second half-reaction. On the basis of their results, they concluded that while a protonated oxygen-centered radical (ie., =NHO•+) was slightly more stable, it was more likely that a protonated nitrogen-centered radical (ie., =NOH•+) is formed during the second half-reaction. This is supported by the formation of **4** as part of the lowest energy pathway outlined above.

As might be anticipated based on the structure of **4**, its lowest energy reaction corresponds to transfer of the proton of the substrate's =NOH•+ group onto O$_{out}$ of the Fe$_{heme}$—O$^{(-)}$OH moiety. This step proceeds via **TS4^1** and **TS4^3** at a cost of 8.7 and 10.0 kcal mol^{-1}, respectively, and results in cleavage of the HO$_{out}$—O$_{in}$ bond with release of O$_{out}$ as H$_2$O and concomitant formation of a compound I-type (Fe$^{IV}_{heme}$=O) species (Figure 4). We note that the singlet pathway is again slightly preferred. The resulting singlet (**5^1**) and triplet (**5^3**) product complexes have essentially the same energy, the triplet being negligibly lower by just 0.1 kcal mol^{-1}. Importantly, however, they are markedly lower in energy than **4^1** by 21.7 and 21.8 kcal mol^{-1}, respectively, and furthermore are also lower in energy than the Fe$_{heme}$—(H)OOH complexes **3^1** and **3^3** (Figure 3).

In **5^1** there is again a radical predominantly localized on the substrate's —NO group (Figure 4). However, now it is predicted to be slightly more oxygen centered (N = −0.36; O = −0.48). In addition, the Fe$_{heme}$—O oxygen also has marked radical nature with a calculated spin density of 0.78. The Fe center has a

calculated spin density of 1.33, slightly higher than the Fe(III) centers in **3^1** (1.04) and **4^1** (1.00) but decidedly lower than the Fe(IV) center (1.97) of **3B^1** (cf. Figure 2). There also appears to be a radical located on the sulfur as indicated by a calculated spin density of −0.71 (see Figure 4). Structurally, on going from **4^1** to **5^1**, the Fe$_{heme}$—O bond has shortened significantly by 0.299 Å to 1.650 Å while conversely, the Fe$_{heme}$—S bond has lengthened considerably by 0.282 Å to 2.621 Å (Figure 4). Similar changes were also observed for **5^3**. Such bond lengths have previously been found to be characteristic of compound I-type species.[33−35] It should be noted that in Figures 3 and 5, compound I is shown as typically given in the literature.

The overall pathway described above shows several similarities to enzymatic peroxidase-type mechanisms.[33] Namely, both share a common Fe$^{III}_{heme}$—(H)OOH intermediate. Then, via a "ping-pong" acid—base catalysis mechanism they transfer the —O$_{in}$H— proton to the —O$_{out}$H group, cleaving the O—O bond with concomitant formation of H$_2$O and a compound I species. However, peroxidases typically employ active site amino acid residues (e.g., histidine) in order to catalyze such a proton transfer.[33] In contrast, NOSs appear to utilize the substrate itself for this role, specifically its —NO group.

3.4. Formation of the Final Products, Citrulline + NO. Possible mechanisms were then considered by which the heme-oxo (compound I) component of intermediate complex **5** may react with the substrate derivative to give the final products, citrulline + NO. The schematic PES for the lowest energy pathway obtained for the overall second half-reaction including the final step is illustrated in Figure 5, while the optimized structures for the triplet compound I intermediate **5^3** and corresponding transition structure (**TS5^3**) and product complexes (**6^3**) are given in Figure 6.

As noted above, the singlet (**5^1**) and triplet (**5^3**) states of **5** are calculated to have almost the same relative energy with the triplet lying just 0.1 kcal mol^{-1} lower in energy. However, it is noted that the corresponding quintet state, **5^5** (Figure S2, Supporting Information), lies just 0.6 kcal mol^{-1} higher in energy than **5^3**. For **5^1** the lowest energy pathway (not shown) found at the present level of theory corresponds to attack of the Fe$_{heme}$—O moiety at the substrate's —NO nitrogen center to

(33) Wirstam, M.; Blomberg, M. R. A.; Siegbahn, P. E. M. *J. Am. Chem. Soc.* **1999**, *121*, 10178.
(34) Shaik, S.; de Visser, S. P.; Kumar, D. *J. Biol. Inorg. Chem.* **2004**, *9*, 661.
(35) Shaik, S.; Kumar, D.; de Visser, S. P.; Altun, A.; Thiel, W. *Chem. Rev.* **2005**, *105*, 2279.
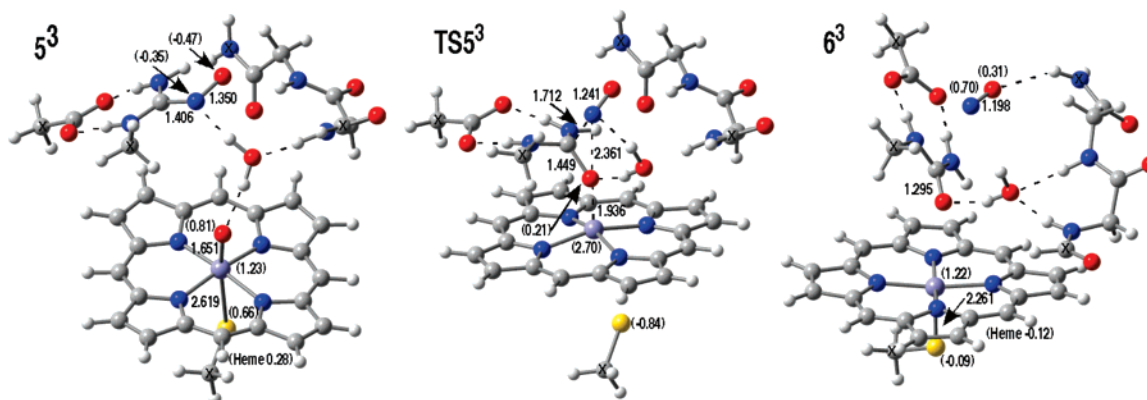
Figure 6. Optimized structures of the triplet state intermediate **5** (**5^3**) and corresponding transition structure (**$TS5^3$**) for formation of the triplet product (**6^3**) complex. Selected optimized distances (Å) and spin densities (in parentheses) are also shown. Color key: Fe (purple); S (yellow); C (gray); N (blue); O (red); H (white).

give an $Fe_{heme}-O-N(O)-$ cross-linked intermediate. However, this reaction was calculated to have a quite high barrier of 23.1 kcal mol^{-1}.

For the triplet (**5^3**) and quintet (**5^5**) states, however, an alternative and markedly lower energy pathway was found. In this alternate mechanism the $Fe_{heme}-O$ oxygen attacks at the substrate's C_{guan} center via a tetrahedral transition structure to directly give the final products citrulline + •NO, i.e., in one-step. For **5^3** and **5^5**, this reaction proceeds via **$TS5^3$** and **$TS5^5$** at a cost of 18.3 and 18.4 kcal mol^{-1}, respectively, to give the corresponding final product complexes **6^3** and **6^5** (Figure 5). These latter complexes lie considerably lower in energy than **5^3** and **5^5** by 50.2 and 51.6 kcal mol^{-1}, respectively. It should be noted that in this present study the "product complex" is the active site with the products of the second half-reaction of NOS (citrulline + NO) remaining bound, along with the H_2O released upon the formation of compound I (Figure 6). The corresponding singlet product complex **6^1** (Table S2, Supporting Information) lies 50.4 kcal mol^{-1} lower in energy than **5^1** and hence is only negligibly lower in energy than **6^3** by 0.1 kcal mol^{-1}.

In the transition structures **$TS5^3$** and **$TS5^5$**, the C–NO bond has lengthened significantly while concomitantly the N–O bond has considerably shortened. For example, in **5^3** the C–NO and N–O bond lengths are 1.406 and 1.350 Å while in the corresponding transition structure **$TS5^3$** they are 1.712 and 1.241 Å, respectively (Figure 6). However, the N–O bond in **$TS5^3$** is still decidedly longer than that of the bound •NO radical (1.198 Å) in **6^3** suggesting that the NO moiety has not yet fully separated from the substrate. In addition, in **$TS5^3$** the forming C–O bond is 1.449 Å long which is similar to that calculated at the same level of theory (data not shown) for the single C–O bond in CH$_3$OH (1.452 Å). However, while the $Fe_{heme}-O$ bond in **$TS5^3$** (1.936 Å) is significantly longer than that in **5^3** (1.651 Å), it has not yet been completely broken. Indeed, it is now close to that observed (1.949 Å) for the $Fe^{III}_{heme}-OOH$ moiety in **4^1** (cf. Figure 4). As noted in the Introduction, most previously proposed mechanisms for the second half-reaction of NOSs have invoked the formation of a tetrahedral intermediate resulting from attack of an $Fe^{III}_{heme}-O_2$ derived species at the substrate's C_{guan} center to give an $Fe_{heme}-O-O-C_{guan}$ peroxo link. However, the results of this present study instead suggest that a tetrahedral $Fe_{heme}-O-C_{guan}$ oxo-linked transition structure is involved.

It is interesting to note that the C–N bond in **5** has substantial double-bond character. For example, in **5^3** $r(C-NO) = 1.406$ Å while the formally single C–N bond length in CH$_3$NO is calculated to be 1.500 Å at the same level of theory (data not shown). In addition, as described in the previous section, the $Fe_{heme}-O$ oxygen of compound I in **5** has marked radical character. Importantly, C=N double bonds are increasingly being recognized as "excellent radical acceptor[s]", particularly those found in oxime ethers (C = NOR).[36] In such cases a radical (R•) attacks and adds at the C=N carbon center to give a nitrogen-centered radical species containing a newly formed C–R bond. The pathway outlined above suggests that NOS may exploit to an extent such an approach. However, in intermediate **5** (Figures 5 and 6) the NHA derivative now contains an –NO• moiety which may represent a more effective leaving group due in part to the inherent stability of the •NO itself in contrast to a •NOR radical species.

It should be noted that the overall mechanism shown in Figure 5 shares some similarities to one previously proposed by Crane and co-workers[14] based on their experimental observations. In particular, they suggested that a compound I species is formed during the second half-reaction but via a P450-type mechanism. Furthermore, they suggested that this then reacts with the substrate to form an oxaziridine species that undergoes an intramolecular rearrangement to give the final products, rather than via a tetrahedral intermediate or transition structure.

4. Conclusions

In this present study we have used density functional theory (DFT) methods in combination with large active-site models in order to investigate the second half-reaction of nitric oxide synthases. Specifically, we first investigated possible reactions of the previously[25] suggested initial mechanism intermediate $Fe_{heme}-(H)OOH$ (**2**). We have then systematically considered possible reactions of the subsequent intermediates in order to elucidate the overall lowest energy pathway leading to the formation of citrulline and NO from NHA. It is noted that the chemical model used in this present study corresponds to one molecule of NHA, an electron and O_2 being added to the active site at the initiation of the second half-reaction. This corresponds

(36) For a recent review see, for example: Miyabe, H.; Ueda, M.; Naito, T. *SYNLETT* **2004**, *77*, 1140 and references therein.

to that which is known from experiments to be consumed during the second half-reaction.

It is found that the lowest energy pathway for the initial mechanism intermediate $Fe_{heme}-(H)OOH$ **2**, formed by transfer of both hydrogens of the NHA substrates $-NHOH^+$ group as previously described,[25] is rotation about the peroxide bond with a very low barrier of just $1-2$ kcal mol^{-1}. This results in the formation of the alternate $Fe_{heme}-(H)OOH$ conformer **3** in which the $-O_{out}H$ proton is now directed down toward the heme porphyrin while the $-O_{in}H-$ group remains hydrogen bonded to the substrate's $-NO$ oxygen. Furthermore, both the singlet and triplet states of **3** (**3¹** and **3³**, respectively) are almost thermoneutral with the initial $Fe^{III}_{heme}-(H)OOH$ intermediate **2** lying just 0.6 kcal mol^{-1} higher in energy. The $Fe_{heme}-O_{in}H-$ proton can then transfer back onto the substrate's $-NO$ oxygen at a cost of 12.2 kcal mol^{-1}. This results in the formation of an $Fe^{III}_{heme}-O(^-)OH$ species while the substrate now contains a terminal $=NOH^{\bullet+}$ group (**4¹**). This latter $=NOH^{\bullet+}$ moiety is then able to transfer its proton to the *outer* oxygen (O_{out}) of the $Fe^{III}_{heme}-O(^-)OH$, resulting in the release of O_{out} as H_2O with concomitant formation of a compound I-type species ($Fe^{IV}_{heme}=O$). This cleavage of the peroxo bond with concomitant proton transfer is found to correspond to the highest overall barrier of the mechanism. For each step in the formation of compound I (**5**), the singlet and triplet states are found to be close in energy with the singlet being slightly preferred.

This pathway is analogous to the ping-pong mechanism by which heme peroxidases can form a compound I species from an initial $Fe_{heme}-(H)OOH$ species. Now, however, the substrate itself appears to play a role in its own oxidation by acting as the amino acid "base species" that such peroxidases commonly use to transfer the proton from the $-O_{in}H-$ to $-O_{out}H$ group.

For the triplet (**5³**) and quintet (**5⁵**) states of the compound I-containing complex (**5**), formation of the final products citrulline and NO is found to be able to occur via a one-step mechanism. Specifically, the $Fe^{IV}_{heme}=O$ oxygen of the compound I moiety, which has marked radical character, attacks at the C_{guan} center of the substrate to form a tetrahedral transition structure containing an $Fe_{heme}-O-C_{guan}$ cross-link at a cost of 18.3 and 18.4 kcal mol^{-1} for the triplet (**TS5³**) and quintet (**TS5⁵**) states, respectively. These transition structures then decompose to directly give citrulline and NO.

Supporting Information Available: Complete citation for reference 28; optimized Cartesian coordinates and calculated energy values for all species in this present study as well as schematic illustration of structures **S1A**, **S1B**, **5⁵**, **TS5⁵**, and **6⁵**. This material is available free of charge via the Internet at http://pubs.acs.org.

JA072650+